$\mathcal{PT}$-symmetric gain and loss in a rotating Bose-Einstein condensate

Daniel Haag,[*] Dennis Dast, Holger Cartarius, and Günter Wunner

Institut für Theoretische Physik 1, Universität Stuttgart, 70550 Stuttgart, Germany

$\mathcal{PT}$-symmetric quantum mechanics allows finding stationary states in mean-field systems with balanced gain and loss of particles. In this work we apply this method to rotating Bose-Einstein condensates with contact interaction which are known to support ground states with vortices. Due to the particle exchange with the environment transport phenomena through ultracold gases with vortices can be studied. We find that even strongly interacting rotating systems support stable $\mathcal{PT}$-symmetric ground states, sustaining a current parallel and perpendicular to the vortex cores. The vortices move through the nonuniform particle density and leave or enter the condensate through its borders creating the required net current.

I. INTRODUCTION

One of the most desired effects studied in Bose-Einstein condensates is the formation of vortices that arise when the condensates are brought into rotation [1]. Vortices were first studied in different low-temperature quantum systems such as superfluid helium [2] and superconductors [3]. In 1961 the Gross-Pitaevskii equation was formulated to describe vortices in a Bose-Einstein condensate [4,5]. Shortly after the first realizations of these ultracold condensates [6,7], Butts and Rokhsar [8] used a variational approach consisting of a linear combination of the low-energy angular-momentum eigenstates of the harmonic oscillator to show that such vortices form themselves if the Bose-Einstein condensate is rotated. Only months later the calculations were experimentally confirmed by Madison *et al.* [9]. At this time, numerical methods such as the finite-element method made the exact numerical study of these systems possible, thus providing a much higher precision [10].

The study of transport phenomena is a common interest in Bose-Einstein condensates, e.g., through optical lattices [11] or even random potentials [12], as well as in superfluids [13,14] and, naturally, in superconductors [15]. If a Bose-Einstein condensate is discussed in the mean-field approximation of the Gross-Pitaevskii equation, the necessary particle gain and loss can be described by imaginary potentials [16], rendering the Hamiltonian non-Hermitian [17]. Up to now, such Hamiltonians have been studied extensively [16,18–23], and the particle in- and out-coupling were compared to many-particle calculations justifying their use in mean-field theory [24,25]. The particle loss can be induced by a focused electron beam [26] while particles are added by letting them fall into the condensate from a second condensate [27].

In 1998 Bender and Boettcher [28] discovered that non-Hermitian Hamiltonians can support stationary solutions if they are $\mathcal{PT}$ symmetric. This finding not only opened the possibility of postulating new theoretical concepts to replace the long accepted requirement of Hermitian Hamiltonians

[29–31] but started many other theoretical and experimental studies in optical [32–40] and electronic systems [41,42]. In these systems, the non-Hermitian Hamiltonian does not describe the full quantum mechanical system but a macroscopic quantity such as the electric field in a wave guide system or the electric current. Inspired by the proposal of Klaiman *et al.* [33], Bose-Einstein condensates were studied as an additional realization using a double-well system, where particles are injected into one well and removed from the other [43–47].

These studies show that $\mathcal{PT}$-symmetric condensates provide an excellent framework for the theoretical study of particle transport through vortex systems. There exists a vast number of numerical and exact analytical calculations, describing stationary vortex states in $\mathcal{PT}$-symmetric systems [48–50]. However, these vortex states are not stable ground states but instead highly excited states. Due to the $\mathcal{PT}$-symmetric potential, the vortex structure of such states is typically lost for strong particle in- and out-coupling.

The formation of vortices in the ground state can be achieved by rotating a nonisotropic trap [51], stirring the condensate [9], or inducing a synthetic magnetic field [52,53]. The different methods all lead to similar equations of motion [9,51,53], one of which is the Gross-Pitaevskii equation in a rotating frame. In natural units and for a rotation axis and angular frequency $(0,0,\Omega)$ it reads

$$
\begin{aligned}
i\frac{\partial}{\partial t}\psi(\boldsymbol{r},t) = [-\Delta + V_{\mathrm{rot}}(\boldsymbol{r}) + 8\pi Na|\psi(\boldsymbol{r},t)|^2 \\
- \Omega\hat{L}_z]\psi(\boldsymbol{r},t),
\end{aligned} \tag{1}
$$

where V_{rot} describes the rotating potential in the rotating frame.

A solution $\psi(\boldsymbol{r},t) = \psi(\boldsymbol{r})\mathrm{e}^{-i\mu t}$ is stationary with respect to the rotating frame and fulfills the stationary rotating Gross-Pitaevskii equation:

$$
\mu\psi(\boldsymbol{r}) = [-\Delta + V_{\mathrm{rot}}(\boldsymbol{r}) + 8\pi Na|\psi(\boldsymbol{r})|^2 - \Omega\hat{L}_z]\psi(\boldsymbol{r}). \tag{2}
$$

Note that for $t = 0$ the wave functions in the rotating and laboratory frame are the same. It can be directly seen that the mean-field energy in the rotating frame differs from the

---

*daniel.haag@itp1.uni-stuttgart.de

nonrotating form, E_{MF}, and reads

$$E_{\mathrm{MF,rot}} = E_{\mathrm{MF}} - \Omega\langle\hat{L}_z\rangle. \qquad (3)$$

If the potential lacks complete rotational symmetry, a nonrotating state can no longer be stationary. The ground state of the system is then determined by the modified mean-field energy $E_{\mathrm{MF,rot}}$ [51], allowing the study of vortex filaments in superfluids and other coherent quantum material.

To solve the stationary rotating Gross-Pitaevskii equation we employ the finite-element method described in Ref. [54]. The three-dimensional wave function is approximated by product states of cubic or higher-order B-splines. To achieve more accurate results, the knots defining the splines are placed recursively such that the error of the kinetic part is minimized. The final number of splines per dimension is reached when the approximated error lies beyond the accuracy of reading on the resulting figure. Depending on the state and the B-spline order, 20 to 60 splines are required per dimension.

Before discussing our numerical results, we have to emphasize that since the potential is time independent in the rotating frame it rotates with the same frequency as the condensate. In particular in the case of potentials that are not isotropic in the rotating plane, this must be considered.

In Sec. II a two-dimensional study of a rotating $\mathcal{PT}$-symmetric potential is conducted. To study particle transport along the vortices, a three-dimensional investigation is performed in Sec. III, followed by a short conclusion in Sec. IV.

II. TWO-DIMENSIONAL SYSTEM

Due to the enormous numerical advantage it is reasonable to start with two-dimensional calculations, i.e., the lowest dimensional system that can provide states with vortices. Effectively two-dimensional condensates are routinely realized in experiments [55–57]. We consider a rotational invariant harmonic trap. In this case, the rotating Gross-Pitaevskii equation in two dimensions assumes the form

$$\mu\psi(x,y) = \left[-\Delta + \tfrac{1}{4}(x^2 + y^2)\right.$$
$$\left. + 8\pi N a_{\mathrm{e}}|\psi(x,y)|^2 - \Omega\hat{L}_z\right]\psi(x,y), \qquad (4)$$

where a modified interaction strength $8\pi N a_{\mathrm{e}}$ appears due to the reduced dimension; its exact value depends strongly on the physical system that is simulated. For the sake of readability, this distinction between the two-dimensional and three-dimensional interaction strengths is dropped in the remainder of the section.

To describe the in- and out-coupling of particles the $\mathcal{PT}$-symmetric imaginary potential

$$V_I(y) = -i\gamma\,\mathrm{sgn}(y) \qquad (5)$$

is used. For positive values of γ the potential describes a gain of particles for $y < 0$ and a loss of particles for $y > 0$. The potential is constant in both regions. This ensures that the same amount of particles is coupled in and out of the system for every possible $\mathcal{PT}$-symmetric wave function. Thus, a comparison between different parameter sets and different numbers of vortices is directly possible. It must be emphasized that the potential is used inside the rotating frame and therefore is itself rotating around the point $x = y = 0$, i.e., the gain and loss
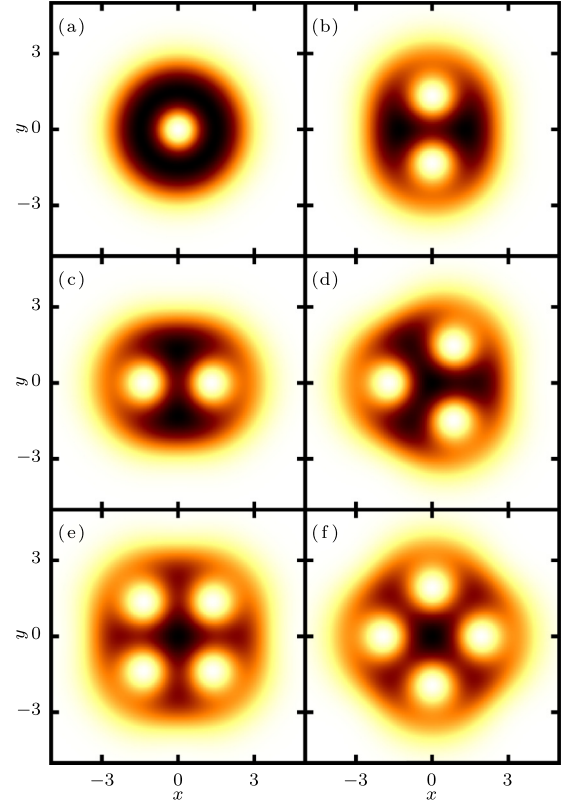

FIG. 1. Ground states of the rotating isotropic harmonic oscillator without gain and loss ($\gamma = 0$) for $\Omega = 0.85$ (a), $\Omega = 0.88$ (b, c), $\Omega = 0.91$ (d), $\Omega = 0.94$ (e, f) in all possible y-symmetric configurations. Note that the states with two, three, and four vortices exhibit a two-, three-, and fourfold symmetry instead of full rotational symmetry. The interaction strength is fixed to $Na = 1$.

contributions are rotating alongside the wave function. This poses an additional challenge to any experimental realization. While particle losses can easily be rotated, the gain requires a more subtle adaption by, e.g., steering the falling atoms or by simultaneously rotating the feeding condensate.

The starting point of this discussion is the case $\gamma = 0$ of an isolated system. For the two-dimensional analysis performed in this section the strength of the nonlinearity is fixed to $Na = 1$. To reveal the multiple vortex ground states predicted by Butts *et al.* [8] various vortex configurations were created to act as initial values for the nonlinear root search used in the finite-element method. Using imaginary time propagation and careful tracing of all branches of solution found, we identified a total of six different ground states in the range of the rotation frequency from $\Omega = 0$ to $\Omega = 0.94$. Four of these states are shown in Fig. 1, possessing one [v_1 in (a)], two [v_2 in (b, c)], three [v_3 in (d)], or four [v_4 in (e, f)] vortices. These states, with the exception of the state with one central vortex, v_1, do not have rotational symmetry but instead show a two-, three- and fourfold symmetry, respectively. For the sake of completeness we note that in the parameter regime discussed in this section, an additional ground state with four vortices but twofold symmetry can be observed for $\Omega = 0.9315$. Applying higher rotation frequencies, the number of vortices would increase even further, until hexagonal vortex grids can be observed [1].
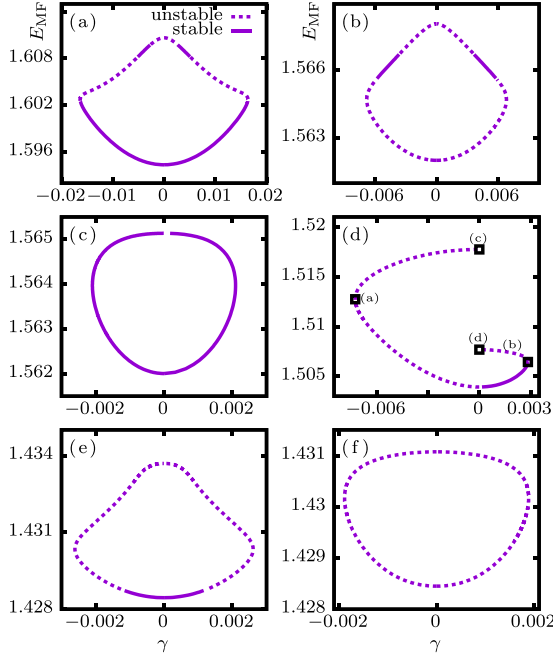
FIG. 2. Mean-field energy of the four ground states v_1 at $\Omega = 0.85$ (a), v_2 at $\Omega = 0.88$ (b, c), v_3 at $\Omega = 0.91$ (d), and v_4 at $\Omega = 0.94$ (e, f) for $Na = 1$ as a function of the in- and out-coupling strength γ. The orientations are chosen in the same way as presented in Fig. 1. While both ground states with two vortices on a central axis parallel to the current are unstable for any $\gamma \neq 0$ (b, f), all other configurations show stable stationary ground states in some parameter regimes. All spectra with the exception of the state v_3 (d) are even functions of γ. Inside the spectra of the state v_3 (d), the two tangent bifurcations and the involved states at the parameter $\gamma = 0$ are marked as a reference for Fig. 3.

By switching on the $\mathcal{PT}$-symmetric potential (5), the stationary states v_1, v_2, v_3, and v_4 become subject to a gain and loss of particles. The imaginary part of the potential, and therefore the particle exchange, rotates concurrently with the wave function. The $\mathcal{PT}$-symmetric potential at $t = 0$ induces a current in the y direction. Real eigenvalues and stable behavior can therefore be expected only if the particle density at $\gamma = 0$ is symmetric with respect to the reflection $y \rightarrow -y$. Figure 1 shows all possible orientations of the four states that fulfill this requirement.

The stability of all states is analyzed via the Bogoliubov–de Gennes equations in the rotating frame:

$$[-\Delta + V(\boldsymbol{r}) - \mu - \omega + 16\pi Na|\psi_0(\boldsymbol{r})|^2 - \Omega\hat{L}_z]u(\boldsymbol{r})$$
$$+ 8\pi Na\psi_0^2(\boldsymbol{r})v(\boldsymbol{r}) = 0, \tag{6a}$$

$$[-\Delta + V^*(\boldsymbol{r}) - \mu^* + \omega + 16\pi Na|\psi_0(\boldsymbol{r})|^2 + \Omega\hat{L}_z]v(\boldsymbol{r})$$
$$+ 8\pi Na\psi_0^{*2}(\boldsymbol{r})u(\boldsymbol{r}) = 0. \tag{6b}$$

The mean-field energy of the four ground states is shown together with their dynamical stability in Fig. 2. The most prominent feature of these spectra is that most of them are even functions of γ. This is a consequence of their symmetry, which can be seen as follows. A reflection of both coordinates x and y obviously leaves the Gross-Pitaevskii equation (4) invariant
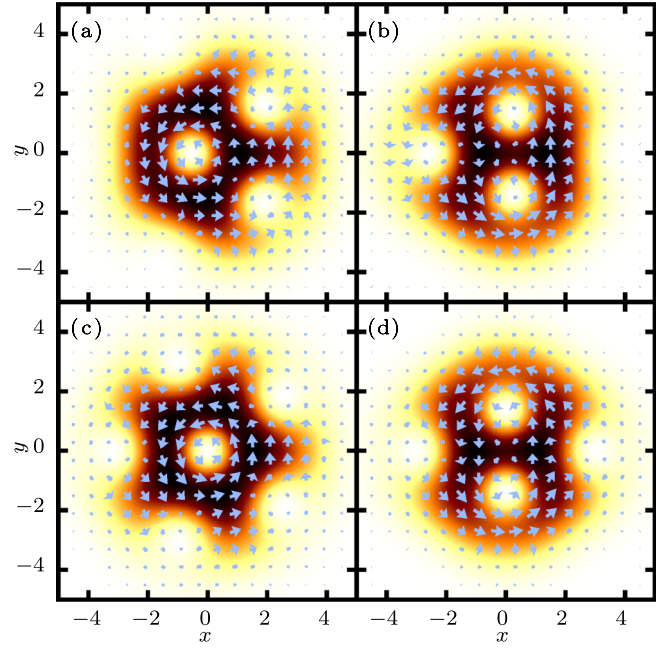

FIG. 3. Wave functions marked in the spectra of the state v_3 for $\Omega = 0.91$ and $Na = 1$ shown in Fig. 2(d). The two states at the bifurcations for negative (a) and positive (b) values of γ are shown above the respective bifurcation partners (c) and (d) taken at $\gamma = 0$. The particle density is shown as a color map, in which darker regions correspond to higher densities, while the currents are depicted by bright blue arrows. Their lengths are proportional to the current strength.

if the wave function itself is invariant under this operation. However, the reflection in the y direction inverts the imaginary potential (5) and can be absorbed in the transformation $\gamma \rightarrow -\gamma$. Therefore, every state that is symmetric in the x direction for $\gamma = 0$ must have an eigenvalue spectrum that is symmetric with respect to $\gamma = 0$.

All ground states exist up or down to some critical value γ where they coalesce with excited states and vanish (inverse tangent bifurcation). This is the typical behavior known from $\mathcal{PT}$-symmetric systems. However, due to the vortices, it is not *a priori* clear what drives the necessary current, i.e., how the necessary phase gradient is generated. To understand the principles of this mechanism the case v_3 is studied in more detail. Figure 2(d) clearly shows that there are two bifurcation partners and two tangent bifurcations. The two states at the bifurcations and the bifurcation partners for $\gamma = 0$, as marked in Fig. 2(d), are shown in Fig. 3. For each state not only the square modulus of the wave function is analyzed but also the particle current density in the nonrotating frame is studied in detail to understand how the currents around the vortices contribute to the net current enforced by the particle gain and loss.

For negative values of γ the net current in the wave function (a) must run downward. This behavior is produced by shifting all three vortex centers to the right while keeping the overall particle density mostly intact. This results in a situation where the current in downward direction on the left side of the wave function is strongly enhanced due to the stronger density. The exact opposite behavior can be found in the case of positive

values of γ, where all vortices shift to the left increasing the net current upward (b).

This is, however, not the only mechanism that changes the net current of these vortex states. A second mechanism can be seen when analyzing, how the excited states shown in Figs. 3(c) and 3(d) behave between $\gamma = 0$ and the bifurcation [Figs. 3(a) and 3(b)]. In complete contrast to the behavior of the ground state, not all vortices are shifted equally strongly. Instead, some vortices are shifted more strongly, completely moving out of the condensate. This increases the current on this side of their neighboring vortices producing an effective current in the upward or downward direction.

For the sake of brevity, we omit a detailed discussion of the other five configurations. A in-depth study shows that these two effects capture almost every current production found in the discussed ground states. In some cases, like the central vortex state v_1, the net current is produced by weakening the undesired current by a new vortex. In other cases, such as the configuration in Fig. 1(c) of two vortices lying on the symmetry axis, both mechanisms are found nearly canceling each other out. In this case the wave function must undergo a serious transformation even though the net currents are very weak. The bifurcation partners, analyzed at $\gamma = 0$, cannot have only a different number of vortices but may also be asymmetric with respect to the reflection $x \rightarrow -x$.

The results show some similarities to the results of Ref. [48], where $\mathcal{PT}$-symmetric bifurcation partners of highly excited nonlinear vortex states are always states with one vortex more or less. However, in contrast to that work and due to the rotation contribution in our calculations, the vortex configurations are much more stable, and vortices emerge only from the wave functions border and not out of a nodal plane.

III. THREE-DIMENSIONAL SYSTEM

Until now, the current always ran perpendicular to the vortex lines. This is a consequence of the restriction to two dimensions. In this section, a net current in direction of the vortices is considered. If the gain and loss of particles is homogeneous in the x-y plane and varies only in the z direction, the imaginary part of the potential does not even need to rotate. To study a current in this direction the z dimension cannot be neglected and the trapping potential cannot be as tight. We therefore choose an isotropic harmonic oscillator:

$$V(r) = \tfrac{1}{4}r^2. \tag{7}$$

The imaginary potential

$$V_I(z) = -i\gamma \, \text{sign}(z) \tag{8}$$

with positive values of γ implements a gain of particles below the x-y-plane and a loss of particles above. The imaginary part of the potential is again constant in each of these regions to ensure that an equal amount of particles is coupled in and out of the system for any shape of the wave function, of which the particle density is at least symmetric under the transformation $z \rightarrow -z$.

To gain access to numerical results, the finite-element method must be provided with initial values for its root search. As long as one is interested in the ground state of the system, excitations in the z direction can be excluded from
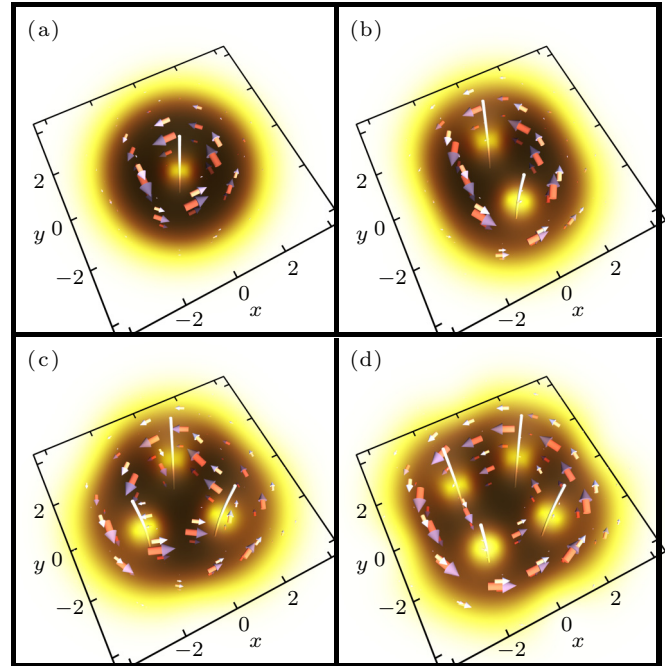

FIG. 4. The particle density of the four ground states in three dimensions with one to four vortices is shown as a color map, in which darker regions correspond to higher densities, and the currents are depicted by bright blue-headed arrows. The vortex centers are highlighted by white lines. For $\Omega = 0.85$ (a) one central vortex exists, while for $\Omega = 0.87$ (b), $\Omega = 0.9$ (c), and $\Omega = 0.94$ (d) all vortices are located off center.

this search. A good approximation to the three-dimensional wave function can therefore be found using a product state of the two-dimensional solution in the x and y directions and a Gaussian ground state in the z direction.

However, to reliably postulate initial values for the ground state the two- and three-dimensional systems must be comparable to start with. Since the trapping potential in the z direction is much weaker than in the two-dimensional case, the modulus square of the mean-field wave function is smaller. To counterbalance this effect the particle number is increased to $Na = 5$. The Gross-Pitaevskii equation then reads

$$\mu\psi(\boldsymbol{r}) = \left[-\Delta + \tfrac{1}{4}r^2 - i\gamma \, \text{sgn}(z) \right.$$
$$\left. + 40\pi|\psi(\boldsymbol{r})|^2 - \Omega\hat{L}_z\right]\psi(\boldsymbol{r}). \tag{9}$$

We start by presenting the rotating ground states for four different rotation frequencies in Fig. 4. As in Sec. II all wave functions are shown in the nonrotating laboratory system at time $t = 0$. Therefore the figure reveals an overall circular current of particles that is consistent with the rotation of the wave function. The concrete path of a vortex core in the z direction is defined by its nodal line. To permit a clear view on this path, the nodal line is highlighted by white lines. Special attention should be given to the state with three vortices in Fig. 4(c). Around $z = 0$ the vortex lines are bent inward towards the rotation center. This effect, even though most distinct at (c), is present in all three wave functions with vortices outside the rotation center. This can be understood since the Magnus force, which keeps the vortices on their
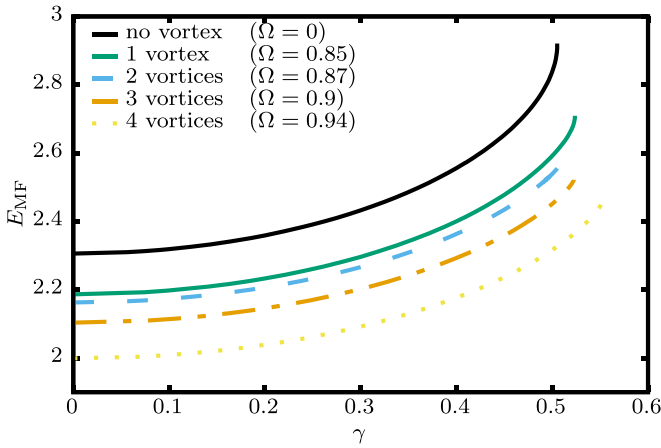
FIG. 5. Mean-field energy of the ground states with zero to four vortices. The in- and out-coupling parameter γ is increased until the mean-field energy undergoes a tangent bifurcation, at which the states vanish. The bifurcation partners are not shown and correspond to the same states with an additional excitation in the z direction.

circular track during the rotation, is stronger for regions of higher particle density, i.e., the density gradient and therefore the Magnus force [58] is increased.

By increasing the parameter γ, the in- and out-coupling drives a new current in the system; particles now have to be transported upward parallel to the vortices. In the case of the unrotated ground state and the four states discussed in Fig. 4 this leads to an increase of the mean-field energy, as shown in Fig. 5. The first eye-catching result of this analysis is that all these ground states behave qualitatively the same. In fact, the bifurcation scenario resembles the behavior of the double-well system or the harmonic oscillator studied in previous investigations [44,45]. All states break the $\mathcal{PT}$ symmetry shortly after $\gamma = 0.5$ in a typical tangent bifurcation. The solutions of the Bogoliubov–de Gennes equations (6) show that they are stable up to this point.

Since the rotation, controlled by the parameter Ω, changes the wave function considerably, not only by increasing or decreasing the number of vortices but also by broadening the wave function, this similarity is quite surprising. It indicates that the x-y plane and the z dimension are only weakly coupled, even though the nonlinearity already provides a major contribution to the planar solutions.

At the bifurcation point the wave functions support the strongest possible current upward. Figure 6 shows these wave functions for the same states as in Fig. 4. Two important effects are visible in these wave functions with maximum current: First, the number and position of the vortices in the x-y plane are changing. This is easy to see in Fig. 6(d). Not only have four new vortices entered the picture, but the original vortices are pushed much tighter together. The new vortices have also increased the size of the wave function. This effect would be expected if either the rotation frequency is increased or the interaction strengthened. Due to the $\mathcal{PT}$-symmetric current in the z direction this component of the wave function cannot be chosen exactly symmetric, i.e., it does not take the shape of a Gaussian. Instead, an antisymmetric contribution is needed, considerably reducing the modulus square at $z = 0$.
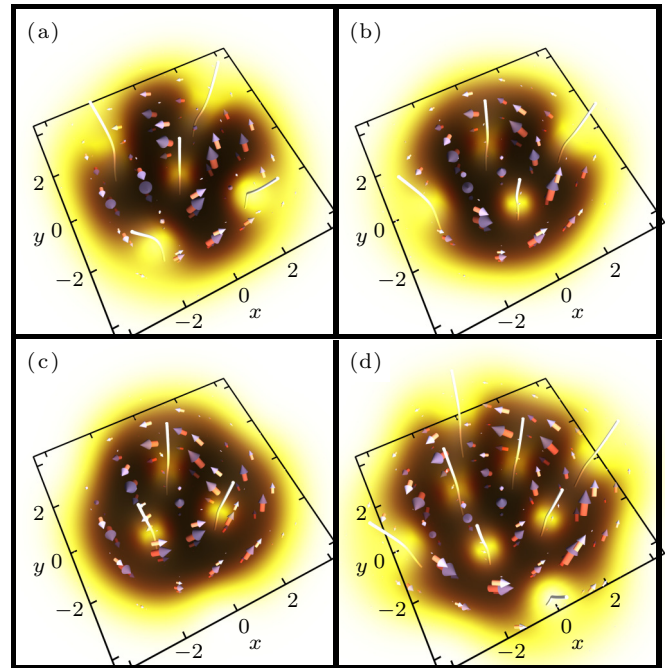

FIG. 6. The four ground states with one to four vortices after evolving to their maximum γ. The particle density is shown as a color map, in which darker regions correspond to higher densities, and the currents are depicted by bright blue-headed arrows. The vortex centers are highlighted by white lines. Additional vortices are added to the ground state at $\Omega = 0.85$ and $\gamma = 0.52$ (a), $\Omega = 0.87$, $\gamma = 0.5$ (b), and $\Omega = 0.94$, $\gamma = 0.54$ (d). The three vortex state $\Omega = 0.9$, $\gamma = 0.51$ (c) is mainly unchanged.

The particles are then forced to the top and bottom of the trap, increasing the particle density and the effective strength of the interaction at these areas.

Second, the previously discussed bending to the center of the trap is not the only deformation of the vortex lines. Following the direction of the $\mathcal{PT}$-symmetric current upward, the vortex lines are screwed in clockwise direction, i.e., against the direction of the frame's rotation. To quantify this screwing, each vortex must be parametrized by the coordinate z in cylindrical coordinates $r(z), \phi(z)$. The vortex screwing is then purely described by the function $\phi(z)$, which is antisymmetric with respect to the x-y plane; the differential $d\phi/dz|_{z=0}$ defines a screwing strength. This value is shown in Fig. 7 as a function of γ.

The shape of all these functions are very similar. In fact, only the maximum reachable γ and the overall slope differ. The different maximum parameters γ are an obvious consequence of the different positions of the tangent bifurcations at which the ground states vanish. The different slopes are best visible for small parameters γ. In this regime, two qualitative dependencies are visible: First, the central vortex is not bent at all. Second, in a stationary state with n noncenter vortices they are screwed m/n times as strong as in the case of m vortices.

This fact indicates that the vortex screwing supports the upward current in the system and each vortex makes an equal contribution. The strongest screwed vortices are therefore found in the two-vortex case. For stronger gain and loss new
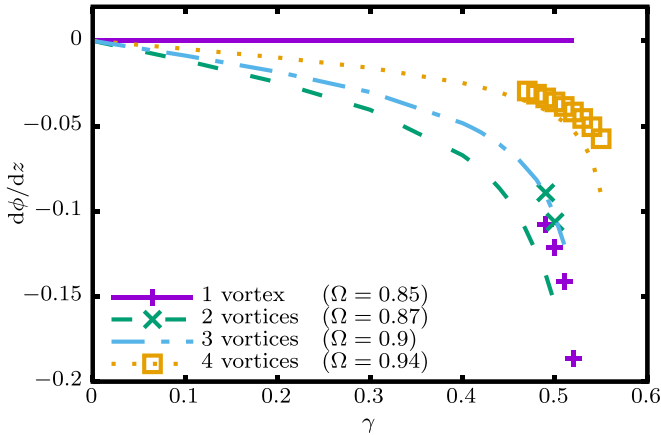
FIG. 7. The screwing strength given as $d\phi/dz|_{z=0}$ of the parametrized vortices, as a function of γ and for different rotation frequencies Ω. The original vortices existing from $\gamma = 0$ upward are shown as lines, and the new vortices arising for larger parameters γ are depicted as different points. Note that all vortices of the same type and from the same wave function are shifted equally.

noncenter vortices arise, depicted as crosses in Fig. 7. In the case of the central vortex state, these new vortices are the only screwed vortices in the wave function. However, in the other two cases the additional vortices are screwed less than the original ones.

IV. CONCLUSION

We studied a rotating Bose-Einstein condensate with a $\mathcal{PT}$-symmetric potential describing particle in- and out-coupling. Initially, the particle transport through the ground state with multiple vortices was studied for the two-dimensional case where the net currents run perpendicular to the rotation axis, i.e., the vortex lines. Not only do most of the states remain

stable, at least for weak currents, but the states producing such currents exhibit interesting behavior. Either new vortices enter the condensate from the border, weakening parts of the circular currents around existing vortices, or the existing vortices move through the nonhomogeneous particle distribution to modify the effective currents.

Both effects obviously arise from the finite size of the condensate, i.e., the drop of the density at its borders. Therefore, it would be worthwhile to study whether the transport phenomena described by $\mathcal{PT}$-symmetric in- and out-coupling are indeed dominated by border currents and border effects of the condensate. The next step would be the study of a larger condensate with constant trapping potential and a bigger vortex grid.

In the next part we added the third dimension to study currents parallel to the rotation axis, i.e., in direction of the vortex lines. In the two-dimensional study weak perpendicular currents sufficed to modify the vortex structure substantially. This changes drastically in the three-dimensional case, in which even strong parallel currents do not break the $\mathcal{PT}$-symmetry. However, the trajectory of the vortex lines in the stable ground states changes. Stronger particle in- and out-coupling strengths lead to a screwing of the vortex lines against the direction of the rotation.

There are various starting points for future studies. While an additional analysis of the stationary system could provide insight into the physical process that leads to the screwing, dynamical calculations will allow us to study how the system behaves when turning on the particle transport. Since the screwed states are stable, the ground state without particle gain and loss can be considered being a small perturbation to the screwed case, and we expect that the current excites oscillations of the vortex lines. For example, it should be possible to study the process in the framework of the dynamics of single vortices in superfluids [58–60] and discuss whether the screwing can be understood as a result of the Magnus force.

[1] A. L. Fetter, Rev. Mod. Phys. **81**, 647 (2009).

[2] R. Feynman, Prog. Low Temp. Phys. **1**, 17 (1955).

[3] A. A. Abrikosov, Sov. Phys. JETP **5**, 1174 (1957).

[4] L. P. Pitaevskii, Sov. Phys. JETP **13**, 451 (1961).

[5] E. P. Gross, Nuovo Cimento **20**, 454 (1961).

[6] K. B. Davis, M.-O. Mewes, M. R. Andrews, N. J. van Druten, D. S. Durfee, D. M. Kurn, and W. Ketterle, Phys. Rev. Lett. **75**, 3969 (1995).

[7] M. H. Anderson, J. R. Ensher, M. R. Matthews, C. E. Wieman, and E. A. Cornell, Science **269**, 198 (1995).

[8] D. A. Butts and D. S. Rokhsar, Nature (London) **397**, 327 (1999).

[9] K. W. Madison, F. Chevy, W. Wohlleben, and J. Dalibard, Phys. Rev. Lett. **84**, 806 (2000).

[10] W. Bao, Ground states and dynamics of rotating Bose-Einstein condensates, in *Transport Phenomena and Kinetic Theory: Applications to Gases, Semiconductors, Photons, and Biological Systems*, edited by C. Cercignani and E. Gabetta (Birkhäuser, Boston, 2007), pp. 215–255.

[11] D.-I. Choi and Q. Niu, Phys. Rev. Lett. **82**, 2022 (1999).

[12] D. Clément, A. F. Varón, M. Hugbart, J. A. Retter, P. Bouyer, L. Sanchez-Palencia, D. M. Gangardt, G. V. Shlyapnikov, and A. Aspect, Phys. Rev. Lett. **95**, 170409 (2005).

[13] S. J. Putterman, *Superfluid Hydrodynamics* (North-Holland, Amsterdam, 1974).

[14] C. J. Pethick, H. Smith, and P. Bhattacharyya, Phys. Rev. B **15**, 3384 (1977).

[15] A. Campbell and J. Evetts, Adv. Phys. **21**, 199 (1972).

[16] Y. Kagan, A. E. Muryshev, and G. V. Shlyapnikov, Phys. Rev. Lett. **81**, 933 (1998).

[17] N. Moiseyev, *Non-Hermitian Quantum Mechanics* (Cambridge University Press, Cambridge, 2011).

[18] P. Schlagheck and T. Paul, Phys. Rev. A **73**, 023619 (2006).

[19] K. Rapedius and H. J. Korsch, J. Phys. B **42**, 044005 (2009).

[20] K. Rapedius, C. Elsen, D. Witthaut, S. Wimberger, and H. J. Korsch, Phys. Rev. A **82**, 063601 (2010).

[21] F. K. Abdullaev, V. V. Konotop, M. Salerno, and A. V. Yulin, Phys. Rev. E **82**, 056606 (2010).

[22] Y. V. Bludov and V. V. Konotop, Phys. Rev. A **81**, 013625 (2010).

[23] D. Witthaut, F. Trimborn, H. Hennig, G. Kordas, T. Geisel, and S. Wimberger, Phys. Rev. A **83**, 063608 (2011).

[24] K. Rapedius, J. Phys. B **46**, 125301 (2013).

[25] D. Dast, D. Haag, H. Cartarius, and G. Wunner, Phys. Rev. A **90**, 052120 (2014).

[26] T. Gericke, P. Wurtz, D. Reitz, T. Langen, and H. Ott, Nat. Phys. **4**, 949 (2008).

[27] N. P. Robins, C. Figl, M. Jeppesen, G. R. Dennis, and J. D. Close, Nat. Phys. **4**, 731 (2008).

[28] C. M. Bender and S. Boettcher, Phys. Rev. Lett. **80**, 5243 (1998).

[29] C. M. Bender, D. C. Brody, and H. F. Jones, Phys. Rev. Lett. **89**, 270401 (2002).

[30] A. Mostafazadeh, J. Phys. A **41**, 055304 (2008).

[31] A. Mostafazadeh, Int. J. Geom. Methods Mod. Phys. **07**, 1191 (2010).

[32] R. El-Ganainy, K. G. Makris, D. N. Christodoulides, and Z. H. Musslimani, Opt. Lett. **32**, 2632 (2007).

[33] S. Klaiman, U. Günther, and N. Moiseyev, Phys. Rev. Lett. **101**, 080402 (2008).

[34] Z. H. Musslimani, K. G. Makris, R. El-Ganainy, and D. N. Christodoulides, Phys. Rev. Lett. **100**, 030402 (2008).

[35] K. G. Makris, R. El-Ganainy, D. N. Christodoulides, and Z. H. Musslimani, Phys. Rev. Lett. **100**, 103904 (2008).

[36] K. G. Makris, R. El-Ganainy, D. N. Christodoulides, and Z. H. Musslimani, Phys. Rev. A **81**, 063807 (2010).

[37] A. Guo, G. J. Salamo, D. Duchesne, R. Morandotti, M. Volatier-Ravat, V. Aimez, G. A. Siviloglou, and D. N. Christodoulides, Phys. Rev. Lett. **103**, 093902 (2009).

[38] C. E. Rüter, K. G. Makris, R. El-Ganainy, D. N. Christodoulides, M. Segev, and D. Kip, Nat. Phys. **6**, 192 (2010).

[39] B. Peng, Ş. K. Özdemir, F. Lei, F. Monifi, M. Gianfreda, G. L. Long, S. Fan, F. Nori, C. M. Bender, and L. Yang, Nat. Phys. **10**, 394 (2014).

[40] A. Regensburger, C. Bersch, M.-A. Miri, G. Onishchukov, D. N. Christodoulides, and U. Peschel, Nature (London) **488**, 167 (2012).

[41] J. Schindler, A. Li, M. C. Zheng, F. M. Ellis, and T. Kottos, Phys. Rev. A **84**, 040101 (2011).

[42] N. Bender, S. Factor, J. D. Bodyfelt, H. Ramezani, D. N. Christodoulides, F. M. Ellis, and T. Kottos, Phys. Rev. Lett. **110**, 234101 (2013).

[43] H. Cartarius, D. Haag, D. Dast, and G. Wunner, J. Phys. A **45**, 444008 (2012).

[44] H. Cartarius and G. Wunner, Phys. Rev. A **86**, 013612 (2012).

[45] D. Dast, D. Haag, H. Cartarius, G. Wunner, R. Eichler, and J. Main, Fortschr. Phys. **61**, 124 (2013).

[46] D. Dast, D. Haag, H. Cartarius, J. Main, and G. Wunner, J. Phys. A **46**, 375301 (2013).

[47] D. Haag, D. Dast, A. Löhle, H. Cartarius, J. Main, and G. Wunner, Phys. Rev. A **89**, 023601 (2014).

[48] V. Achilleos, P. G. Kevrekidis, D. J. Frantzeskakis, and R. Carretero-González, Phys. Rev. A **86**, 013808 (2012).

[49] V. V. Konotop, J. Yang, and D. A. Zezyulin, Rev. Mod. Phys. **88**, 035002 (2016).

[50] L. Schwarz, H. Cartarius, Z. H. Musslimani, J. Main, and G. Wunner, Phys. Rev. A **95**, 053613 (2017).

[51] L. D. Landau and L. P. Pitaevskii, *Statistical Physics, Part 2: Theory of the Condensed State* (Pergamon, Oxford, 1979).

[52] Y.-J. Lin, R. L. Compton, K. Jiménez-García, J. V. Porto, and I. B. Spielman, Nature (London) **462**, 628 (2009).

[53] Q. Zhao and Q. Gu, Front. Phys. **10**, 100306 (2015).

[54] D. Haag, D. Dast, H. Cartarius, and G. Wunner, Int. J. Theor. Phys. **54**, 4100 (2015).

[55] A. Görlitz, J. M. Vogels, A. E. Leanhardt, C. Raman, T. L. Gustavson, J. R. Abo-Shaeer, A. P. Chikkatur, S. Gupta, S. Inouye, T. Rosenband, and W. Ketterle, Phys. Rev. Lett. **87**, 130402 (2001).

[56] H. Saito and M. Ueda, Phys. Rev. Lett. **90**, 040403 (2003).

[57] D. Rychtarik, B. Engeser, H.-C. Nägerl, and R. Grimm, Phys. Rev. Lett. **92**, 173003 (2004).

[58] B. P. Anderson, P. C. Haljan, C. E. Wieman, and E. A. Cornell, Phys. Rev. Lett. **85**, 2857 (2000).

[59] P. G. Kevrekidis, R. Carretero-González, G. Theocharis, D. J. Frantzeskakis, and B. A. Malomed, J. Phys. B **36**, 3467 (2003).

[60] D. J. Frantzeskakis, G. Theocharis, F. K. Diakonos, P. Schmelcher, and Y. S. Kivshar, Phys. Rev. A **66**, 053608 (2002).